

## Modeling and Performance analysis of Metallic CNT Interconnects for VLSI Applications

<sup>1</sup>Y.Amar Babu, <sup>2</sup>G.M.V.Prasad

<sup>1</sup>L.B.R. College of Engineering Mylavaram-521230 Andhrapradesh, India

<sup>2</sup>B.V.C. Institute of Technology & Science Batlapalem-533221 Andhrapradesh, India

---

**Abstract:** THE SEMICONDUCTOR INDUSTRY is confronting an acute problem in the interconnect area as IC feature sizes continually scale below 32 nm. When the cross sectional dimension of copper wires approach their mean free path (about 40 nm at room temperature), they suffer significant size effects because of increasing surface scattering, grain boundary scattering, and the presence of a highly resistive diffusion barrier layer, resulting in a sharp rise in copper resistivity. According to the 2011 International Technology Roadmap for Semiconductors (<http://public.itrs.net>), copper's resistivity could be more than three times higher than its bulk value at the 22-nm technology node. This steep rise in resistivity will adversely impact both performance and reliability in terms of circuit delay, chip temperature, and current-carrying capacity. This limitation of copper interconnects is driving research for alternative interconnect materials and technologies for next-generation ICs. In this research, carbon nanomaterials, with their many attractive properties, are emerging as the frontrunners to potentially replace copper for interconnects and passive devices in ICs, including vias and through-silicon vias (TSVs), horizontal wires (local, intermediate, and global levels) and off-chip interconnects.

---

### I. Introduction

In this paper, we discuss various carbon nanomaterials, along with their prospects for next-generation interconnects and passive devices. We also provide a comparative analysis of these nanomaterials, and we illustrate why carbon nanomaterials constitute the ideal interconnect technology choice for next-generation ICs. Unique properties of carbon nanomaterials Low-dimensional allotropes of carbon, known as carbon nanomaterials, have extraordinary physical properties because of their unique structure. In particular, researchers have extensively investigated their 1D forms, carbon nanotubes (CNTs) and grapheme nanoribbons (GNRs), because of their exciting prospects in various applications, including interconnects and passive devices in the nanoelectronics area<sup>1</sup>.

### II. Atomic structure and properties

To understand the physics of CNTs and GNRs, we need to study their atomic structure. Both CNTs and GNRs can be formed from a single-layer grapheme sheet. The carbon atoms in a grapheme sheet are arranged in a 2D honeycomb lattice structure.

A GNR can be formed by cutting a ribbon out of grapheme following an edge shape (either armchair or zigzag). A CNT can be formed by rolling up a ribbon along circumferential vector  $\vec{C}$  (see Figure 1a). The CNT's chirality is defined using  $\vec{C}$  (the roll-up direction), which is a combination of lattice vectors

$$\vec{C} = n \cdot \hat{a}_1 + m \cdot \hat{a}_2$$

where n and m are a pair of integers known as the chiral indices. Depending on the circumferential edge shape, a CNT can be armchair ( $n = m$ ), zigzag ( $n = 0$  or  $m = 0$ ), as shown in Figure 1a, or chiral (other shapes). On the other hand, a GNR's chirality is defined by the edge shape, which is opposite to that of a CNT. Thus, starting from the same grapheme strip, the CNT shown in Figure 1a is armchair, whereas the GNR is zigzag. The diameter D of the CNTs is also determined by the chiral indices:

$$D = \left| \vec{C} \right| / \pi = \frac{a}{\pi} \sqrt{n^2 + m^2 + mn}$$

where a is the lattice constant of grapheme (0.246 nm). Depending on the number of concentrically rolled up shells, CNTs can be classified as single-walled CNTs(SWCNTs), double-walled CNTs (DWCNTs), or multiwalled CNTs (MWCNTs). Similarly, GNRs can be classified as monolayer, bilayer, or multilayer. The ideal interval distance between different shells in DWCNTs and MWCNTs, or between adjacent layers in multilayer GNRs is the Van der Waal's gap (about 0.34 nm). The unique properties of CNTs and GNRs are largely due to the unique band structure of grapheme, in which the E-k (energy vs. wave vector) relation is linear for the low energies near the six corners of the 2D hexagonal Brillouin zone (as shown in Figure 1b), leading to zero effective mass for electrons and holes.<sup>1</sup> Because of this

linear dispersion relation at low energies, electrons and holes near these six points behave like relativistic particles described by the Dirac equation for spin-1/2 particles.

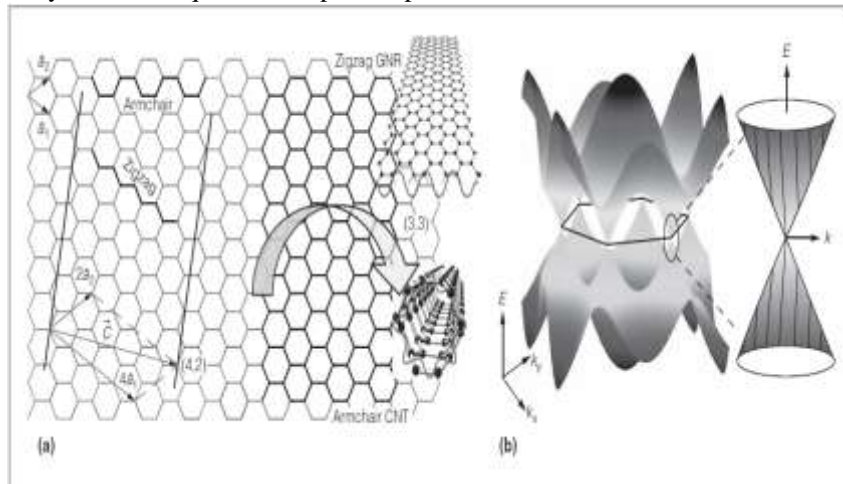


Figure 1. The atomic structure of CNT and GNR derived from a graphene sheet (a), and the band structure of graphene, where the conduction band and valence band meet at the six conical vertices (Dirac points) (b). The left side of (a) shows the chirality definition in terms of lattice vectors  $\hat{a}_1$  and  $\hat{a}_2$ ; the (4, 2) vector is shown as an example. The right side of (a) shows a zigzag-GNR and a (3, 3) armchair CNT based on the same ribbon, along with the schematic view of their wave function quantization. The zoomed-in conical shape on the right side of (b) shows a linear E-k relationship, where E is the energy and k is the wave vector. The wave function quantization leads to the formation of a set of slice cuts on the graphene band structure (the vertical lines on the right conical). If a slice cuts at one conical intersection point, there is no band gap (metallic); otherwise, there is a band gap (semiconducting). The band gap is inversely proportional to the GNR width or the CNT diameter.

Hence, the electrons and holes are called massless Dirac fermions, and the six corners of the Brillouin zone are called the Dirac points. Moreover, the  $sp^2$  bonding in these materials (where s and p are the atomic orbitals), which is stronger than the  $sp^3$  bonds in diamond, makes graphene the strongest material ever measured. CNTs and GNRs also have very high current-carrying capability (at least two orders of magnitude higher than that of copper). In addition, CNTs and GNRs have long mean free paths (MFPs) at low bias because of weak acoustic phonon scattering and suppressed optical phonon scattering at room temperature. Table 1 summarizes the key electrical, thermal, and mechanical properties of carbon nanomaterials relevant to their interconnect and passive applications.<sup>1</sup>

### III. Metallicity of CNTs and GNRs

For interconnect applications, the metallicity of CNTs and GNRs is the main concern. It's important to understand their electronic structure, which again originates from graphene's band structure, as shown in Figure 1b. The band structure of CNTs and GNRs can be studied from that of graphene by considering their structural confinement.

The difference in the confinement conditions between CNTs and GNRs is that the wave function along the CNT circumference is periodic, whereas the wave function along the GNR width vanishes at the two edges (Figure 1a). These confinements can be reflected into the band structure as slice cuts (Figure 1b), each representing one subband. Depending on the position of the slice cuts due to chirality and diameter, the resulting band structure could be without band gap (metallic) or with band gap (semiconducting). Li et al. have explained that the condition for achieving a metallic CNT can be expressed as  $n - m = 3i$ , where i is an integer.<sup>1</sup> Hence, armchair CNTs are always metallic (see Figure 1a), whereas zigzag CNTs could be metallic or semiconducting, depending on the chiral indices (n, m). Statistically, a natural mix of CNTs will have one-third metallic and two-thirds semiconducting chirality. On the other hand, zigzag GNRs are always metallic (a small band gap will be induced in zigzag GNRs once electron spin is considered, because of the staggered sublattice potential from magnetic ordering<sup>1</sup>). Armchair GNRs can be either metallic or semiconducting, depending on the number (N) of atoms across the width: metallic when  $N \neq 3i - 1$ , and semiconducting when  $N = 3i$  or  $3i + 1$ .

Table 1. Properties of carbon nanomaterials relevant to VLSI interconnects and passive applications.

Property	W	Cu	SWCNT	MWCNT	Graphene or GNR
Maximum current density (A/cm <sup>2</sup> )	10 <sup>8</sup>	10 <sup>7</sup>	>10 <sup>8</sup>	>10 <sup>8</sup>	>10 <sup>8</sup>
Melting point (K)	3695	1357		3800 (graphite)	
Density (g/cm <sup>3</sup> )	19.25	8.94	1.3–1.4	1.75–2.1	2.09–2.33 (graphite)
Tensile strength (GPa)	1.51	0.22	22.2 ± 2.2	11 to 63	
Thermal conductivity (×10 <sup>3</sup> W/m·K)	0.173	0.385	1.75 to 5.8	3	3 to 5
Temperature coefficient of resistance (×10 <sup>-3</sup> /K)	4.5	4	<1.1	-1.37	-1.47
Mean free path (nm) at room temperature	33	40	>10 <sup>3</sup>	2.5 × 10 <sup>4</sup>	1 × 10 <sup>3</sup>

\* CNT: carbon nanotube; Cu: copper; GNR: graphene nanoribbon; MWCNT: multiwalled CNT; SWCNT: single-walled CNT; W: tungsten.  
 \*\* All the references for these values reported in this table are listed in Li et al.<sup>1</sup> But these values are valid only for certain CNTs or graphene cases, because they depend on many other parameters, such as CNT diameter and GNR width, or even on different fabrication processes.

#### IV. Modeling and performance analysis

As interest in carbon-nanomaterial-based interconnects gains momentum, a realistic analysis of these interconnects is necessary to evaluate their performance and identify the domains of on-chip interconnections (local, intermediate, and global interconnects or vias) where this novel interconnect technology has the potential to replace copper. Here, we introduce circuit models for various types of CNTs and GNRs, and analyze their performance in various applications.

##### RLC model

Figure 2 shows the proposed RLC-equivalent circuit models for SWCNTs and GNRs. For DWCNT and MWCNT interconnects, a more complicated equivalent circuit is employed. (Li et al. presented a detailed model for MWCNT interconnects, which is also valid for DWCNT interconnects. They also provided a detailed discussion about other CNT and GNR modeling work.) We can derive the conductance of CNTs and GNRs using the linear-response Landauer formula, which takes into account the large quantum contact resistance  $R_Q$  (about 12.9 kΩ per conducting channel) between 1D conductors and 3D materials. Although both CNTs and GNRs are considered 1D materials, a significant difference between them is the existence of edge scattering in GNRs. CNTs are seamless tubular structures, which allow electrons to travel around. GNRs, however, have abrupt edges and induce scattering because of edge roughness. Figure 3a compares the resistances of various CNTs (SWCNTs, DWCNTs, and MWCNTs) and GNRs (monolayer GNRs, neutral multilayer GNRs, and doped multilayer GNRs). For short lengths, due to large quantum contact resistance, the resistance per unit length of CNTs and GNRs are large but decrease with increasing length, and they become stable after 10 nm. For longer lengths, all types of CNTs could offer lower resistance than copper, whereas only AsF<sub>5</sub> (arsenic pentafluoride) intercalation-doped multilayer GNRs with high specularity (or very smooth edges) can provide lower resistance than that of copper. (Intercalation involves inserting a dopant layer between adjacent graphene layers.) Besides quantum contact resistance  $R_Q$ , the RLC model in Figure 2 has two other new circuit elements: quantum capacitance  $C_Q$  and kinetic inductance  $L_K$ . Both of these arise mainly because CNTs and GNRs are low dimensional materials with low density of states near the Fermi level. In materials with low density of states, adding charges to the system not only requires certain electrostatic energy, but also requires non negligible additional energy to occupy the higher energy states. This additional energy can be modeled as the quantum capacitance  $C_Q$  (about 193 aF/nm per channel) in series with electrostatic capacitance  $C_E$ .

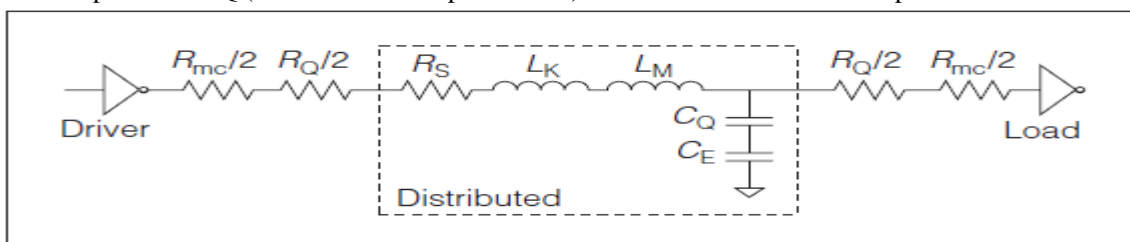


Figure 2. The equivalent distributed RLC circuit model of an SWCNT or GNR interconnect.  $R_{mc}$  is the imperfect contact

resistance between the CNT and the metal; RQ is the quantum contact resistance associated with the contact from the 1D conductor to the 3D conductor; RS is the scattering-induced resistance, depending on mean free path; LK is the kinetic inductance; LM is the magnetic inductance associated with the CNTs or GNRs; and CQ and CE are the quantum and electrostatic capacitances.

Similarly, to establish a current in a system, the number of charges moving in one direction must exceed the charges moving in the other direction. These excess moving charges also require excess energy to occupy higher energy states, and the excess energy associated with the moving charges can be modeled as the kinetic inductance LK (about 8 nH/mm per channel) in series with the conventional magnetic inductance LM. The value of kinetic inductance is about three orders larger than that of magnetic inductance in a single CNT or monolayer GNR. (Other experimental work on the high-frequency characterization of CNTs has verified the existence of kinetic inductance; see the work of Li et al. for details.)

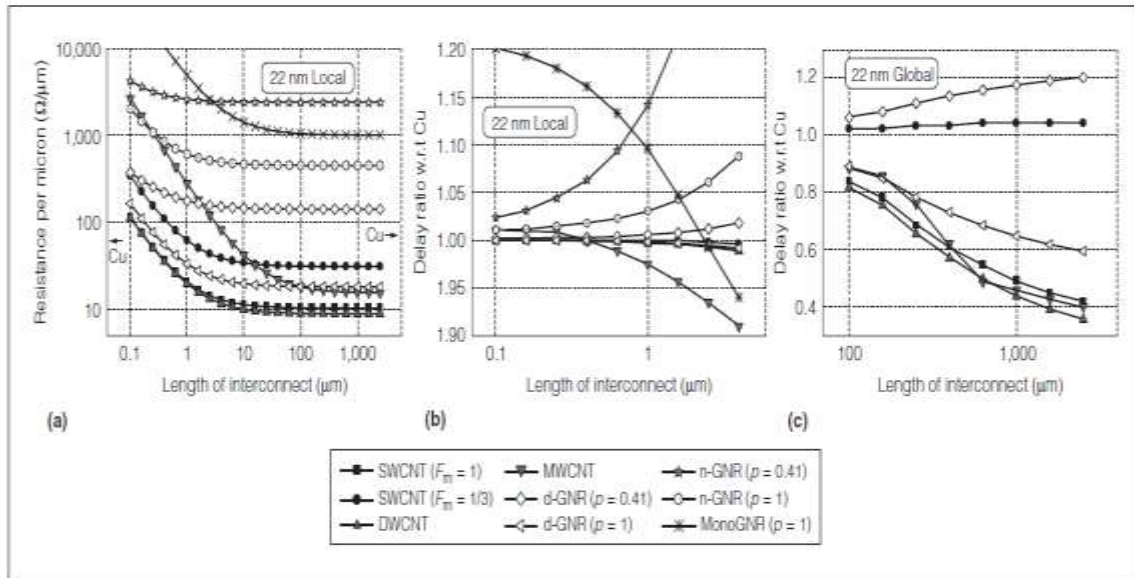


Figure 3. Resistance per unit length comparison for different types of CNT and GNR interconnects for the dimensions

predicted in the 2008 International Technology Roadmap for Semiconductors (<http://public.itrs.net>) for local interconnects at the 22-nm technology node (22-nm width and 44-nm height) (a). Signal delay ratios (with respect to copper) of SWCNT, DWCNT, MWCNT, and different types of GNRs at the 22-nm technology node for local (b) and global (c) interconnects. The driver size is assumed to be 2 in (b) but is set to 100 in (c). The global-interconnect width is set to be five times the minimum width, as predicted by the ITRS.  $F_m$  indicates the fraction of metallic SWCNTs in the SWCNT bundle; n-GNR and d-GNR represent neutral multilayer GNRs and AsF5 (arsenic pentafluoride) intercalationdoped GNRs, respectively; and  $p$  indicates the specularity of a GNR edge:  $p = 1$  indicates no edge scattering (best case), and  $p = 0$  implies a completely diffusive edge (worst case). For the DWCNT, the diameter is set to 1.5 nm, and metallic fraction  $F_m = 1$ . The diameter of the MWCNT and the width of the GNR are equal to the wire width ( $W$ ).

## V. Conclusion:

We've compared the performance of different carbon-nanomaterial-based interconnects with that of copper interconnects on the basis of the model in Figure 2. Figures 3b and 3c show the delay ratios of CNT and GNR interconnects with respect to copper for local- and global-level interconnects at the 22-nm technology node. Metallic CNT interconnects best for global interconnect in VLSI applications.

## References

- [1] H. Li et al., "Carbon Nanomaterials for Next-Generation Interconnects and Passives: Physics, Status, and Prospects," IEEE Trans. Electron Devices, vol. 56, no. 9, 2009, pp. 1799-1821.
- [2] T. Xu et al., "Aligned Carbon Nanotubes for Through-Wafer Interconnects," Applied Physics Letters, vol. 91, no. 4, 2007, article 042108.
- [3] C. Xu et al., "Compact AC Modeling and Analysis of Cu, W, and CNT Based Through Silicon Vias (TSVs) in 3-D ICs," Proc. IEEE Int'l Electron Device Meeting (IEDM 09), IEEE Press, 2009, pp. 521-524.
- [4] J. Li et al., "Bottom-up Approach for Carbon Nanotube Interconnects," Applied Physics Letters, vol. 82, no. 15, 2003, pp. 2491-2493.
- [5] T. Iwai et al., "Thermal and Source Bumps Utilizing Carbon Nanotubes for Flip-Chip High Power Amplifiers," Proc. IEEE Int'l Electron Device Meeting (IEDM 05), IEEE Press, 2005, pp. 257-260.

- [6] K. Korda's et al., "Chip Cooling with Integrated Carbon Nanotube Microfin Architectures," *Applied Physics Letters*, vol. 90, no. 12, 2007, article 123105.
- [7] M. Nihei et al., "Low-Resistance Multi-walled Carbon Nanotube Vias with Parallel Channel Conduction of Inner Shells," *Proc. IEEE Int'l Interconnect Technology Conf. (IITC 05)*, IEEE Press, 2005, pp. 234-236.
- [8] M. Katagiri et al., "Fabrication of 70-nm-Diameter Carbon Nanotube Via Interconnects by Remote Plasma- Enhanced Chemical Vapor Deposition and Their Electrical Properties," *Proc. IEEE Int'l Interconnect Technology Conf. (IITC 09)*, IEEE Press, 2009, pp. 44-46.
- [9] J. Dijon et al., "Carbon Nanotubes for Interconnects in Future Integrated Circuits: The Challenge of the Density," *Diamond and Related Materials*, vol. 19, nos. 5-6, 2010, pp. 382-388.
- [10] D.N. Futaba et al., "Shape-Engineerable and Highly Densely Packed Single-Walled Carbon Nanotubes and Their Application as Super-Capacitor Electrodes," *Nature Materials*, vol. 5, no. 12, 2006, pp. 987-994.
- [11] A.R. Harutyunyan et al., "Preferential Growth of Single- Walled Carbon Nanotubes with Metallic Conductivity," *Science*, vol. 326, no. 5949, 2009, pp. 116-120.
- [12] A. Kawabata et al., "Robustness of CNT Via Interconnect Fabricated by Low Temperature Process over a High- Density Current," *Proc. Int'l Interconnect Technology Conf. (IITC 08)*, IEEE Press, 2008, pp. 237-239.
- [13] Q. Yu et al., "Graphene Segregated on Ni Surfaces and Transferred to Insulators," *Applied Physics Letters*, vol. 93, no. 11, 2008, article 113103.
- [14] X. Li et al., "Large-Area Synthesis of High-Quality and Uniform Graphene Films on Copper Foils," *Science*, June 2009, pp. 1314-1314.
- [15] D. Kondo, S. Sato, and Y. Awano, "Self-Organization of Novel Carbon Composite Structure: Graphene Multilayers Combined Perpendicularly with Aligned Carbon Nanotubes," *Applied Physics Express*, vol. 1, no. 7, 2008, article 074003.